Comparison of three wastewater sludge drying processes: solar, thermal and reed beds - Impact on organic matter characteristics.

Marie Collard, Benoit Teychené, Laurent Lemée*

*Corresponding author

tel : 33 (0)5 49 45 38 92

fax: 33 (0)5 49 45 35 01

e-mail : laurent.lemee@univ-poitiers.fr

Université de Poitiers, CNRS, UMR 7285 (IC2MP), 4 rue Michel Brunet – TSA 51106, 86073 Poitiers Cedex 9, France

Abstract

Drying process aim at minimising the volume of wastewater sludge (WWS) before disposal, however it can impact sludge characteristics. As sludge composition is a major parameter for the choice of disposal techniques, the objective of this study was to observe the influence of solar, reed beds and thermal drying processes on WWS organic matter (OM). WWSs OM from each process were investigated at the global and molecular scales using elemental analysis, infrared spectroscopy, OM fractionation and thermochemolysis.

Changes in global and spectroscopic characteristics were monitored for the three drying processes. A strong influence of drying on lipid and humic-like substances contents was observed through OM fractionation for thermal and solar drying. This traduced a weakening of OM for thermal and a complexification for solar drying. At the molecular scale, no change was observed in the composition but differences appeared within the distributions particularly for thermal drying.

Keywords

Wastewater sludge, drying process, organic matter, lipids, humic-like substances, fractionation, infrared spectroscopy, thermochemolysis-GC/MS,

1.Introduction

Every year large amounts of wastewater sludgeare produced worldwide. In European Union (EU), these amounts are expected to strongly increase up to 13 million tons dry sludge (DS) by 2020 due to the implementation of new urban wastewater treatment directives (Commission of European Communities). Sludge management (e.g. disposal) and treatment represent more than 50 % of the construction and operating costs of a wastewater treatment plant (WWTP) (Pognani et al. 2011). According to several recent reports and as recently reviewed by Kelessidis, sludge management is mainly performed in EU by landfarming (direct or after composting), incineration (after drying) and landfill (Kelessidis and Stasinakis 2012).

While landfill is massively abandoned in EU and with the expected large increase in sludge production, future trends in sludge disposal techniques are expected to be land farming (direct or after composting) and energy recovery processes (Biogas production) in order to reduce energy costs associated to sludge drying and incineration (Kelessidis and Stasinakis 2012; [CSL STYLE ERROR: reference with no printed form.]).

A step of drying is commonly used before land farming. This step aims at reducing the volume of sludge (due to its high water content) and at sanitising. The different ways of drying are natural drying, mechanical drying or thermal drying. Sludge treatment processes generally have two main purposes: 1/ thickening and dewatering whereby the sludge volume, and hence the costs of subsequent handling, transportation and disposal, are reduced (Uggetti et al. 2010), and 2/ stabilisation through microbial decomposition of labile organic matter remaining in the sludge (Lasaridi and Stentiford 1998). Moreover, sludge drying also results in an increase of its calorific value so it can be used as an efficient combustible source (Chai 2007).

Pelletisation is a drying process which aims at producing fertiliser from sewage sludge. The sludge which can contain up to 97% water is pumped from the plant's storage tanks, mixed with a coagulating agent, and pressed with wide fabric belts. The resulting solid, called sludge cake, contains roughly 25% solids and 75% water. This sludge cake is then baked at 120° C in "tumble-drying" ovens that destroy all pathogens and bacteria, remove up to 90% of the remaining water, and rotate the sludge into fertiliser pellets.

Greenhouse drying is a sludge drying process in solar plants. The aim is an acceleration of the water evaporation rate exploiting the artificial green-house effect and avoiding the equilibrium of vapor pressure between sludge and air by controlled indoor air ventilation (Mathioudakis et al. 2013). Moreover, the greenhouse plant drying technology is characterised by a reduced environmental footprint compared to conventional outdoor drying beds method as well as low energy requirements in contrast to conventional thermal dryers (Bux et al. 2002).

Reed bed (RB) systems for sludge dewatering have been reported for over 30 years (Edwards et al. 2001) and are now widely used throughout the world (Nassar et al. 2006). They involve low capital and running costs and represent a good solution for sludge management in small wastewater treatment plants. Typically, a RB system consists of at least 8 beds (Nielsen 2003) planted with common reed (Phragmites australis (Cav.) Trin. Ex Steud). The sludge is distributed evenly over the surface of the beds through a system of loading pipes (Nielsen 2003). The reeds are planted and rooted in a growth layer placed on top of the drainage layer (Nielsen and Willoughby 2005). An underdrain system allows excess water from the sludge to be easily drained, while the sludge accumulates over layers of sand and gravel. The drained water is collected in a system of drainage pipes in the bottom of the beds, which also enhance the aeration of the sludge residue since they are connected to vertical aeration pipes (Uggetti et al. 2010). As sludge builds up in the beds, the reeds will extend their roots into the growing sludge layer. The beds of a RB system are loaded according to the following cycle: one bed is loaded for a period of a few days and then rests for several weeks while the next beds are loaded. The long resting period allows the sludge to dewater through gravity drainage and evaporation (Nielsen 2003). A RB system has a life expectancy of 30 years or more. During this period each bed needs to be emptied every 8–12 years (Nielsen and Willoughby 2005).

The organic matter of WWS is constituted with residues of the influent, microorganisms and extracellular polymer substances (EPS). WWS is thus a complex mixture of proteins, polysaccharides, cellulose, hemicellulose, lipids, macromolecules with both aromatic and aliphatic structures and anthropogenic compounds (micro pollutants, polymers, detergents) (Parnaudeau and Dignac 2007). In addition, as previously demonstrated (Réveillé et al. 2003; Jardé et al. 2003; Jardé et al. 2005a; Parnaudeau and Dignac 2007) the relative amount of each compound is related to the wastewater origin (municipal, industrial, food processing) or to treatment conditions (e.g. composting). Many studies are dedicated to WWS characterisation in terms of global parameters (carbon, nitrogen contents, BOD, etc.) and specific compounds (lipids, proteins, humic-like substances, etc.) (Jardé et al. 2005b), but few studies concern the structural characterisation at a molecular level.

Thermochemolysis-GC/MS is a powerful tool to characterize, at the molecular scale, complex organic mattermixture (Nielsen and Willoughby 2005; Mathioudakis et al. 2013) and its evolution during waste disposal (composting, soil amendment, etc) (González-Vila et al. 2001; Hernández et al. 2002).

The objective of this study was to compare the OM characteristics of WWS which have been submitted to different drying processes. Indeed sludge composition is a key parameter that governs the choice of disposal techniques. For example, energy recovery from bio digester processes strongly depends on OM composition of the WWS (Kwon et al. 2013). Furthermore, sludge intended to be recycled in agriculture have to achieve limited metals (Cd, Cr, Ni, Pb...) and organic compounds (nonylphenol, organic halogens, polychlorinated biphenyls...)(Jardé et al. 2005b) concentrations.

In this study, the remnant organic matter from 3 WWTP was investigated at the global and the molecular scale using elemental analysis, infrared spectroscopy (IRFT) and thermochemolysis (THM). WWS which have been submitted to solar, reed beds and thermal drying were compared at different stages of the processes.

2. Materials and methods

2.1 Description of wastewater treatment plants and sludge line

Three French WWTP located near Poitiers (Vienne, France) were studied.

The WWTP of Poitiers, La Folie (LF) has a nominal capacity of 152,500 population equivalent (PE). Wastewater is collected from a semi-separative network (93 % of the network's length is separative) and the treatment is based on classical activated sludge process (sludge retention time: 48 h) coupled with an intensive phosphate removal step using iron chloride. The WWS is purged from the settling tank and concentrated by flotation (using micro-bubbles) after lime addition (pH: 7.3-7.5) and exhibited a dried matter content ranged from 2.5 to 5 %. After dewatering using filtration, the concentrated sludge (22 % of dry content) is directly composted with green waste or thermally dried to 92-97 % of dried matter and transform into sludge pellets which are incinerated or used as fertilisers (88-92 % of dried matter). Dried sludge is obtained thanks to a thin film conductive drier working at 85°C. The 6 mm pellets are produced using a dryer-pelletizer working at 120°C. The sludge pellets are then stored at ambient temperature before agricultural recycling or incineration. The total sludge production is equal to 1,357 tons of DS/year. Before drying the concentrated sludge is mixed with a cationic polymer (ZETAG, BASF France) at a concentration of 15 kg per ton of DS.

68 % of the total WWS amount is used in co-composting and 32 % is transformed into pellets. 3 treatment steps were sampled for this study: Floated sludge (LF-0), dry sludge (LF-85) and pellets (LF-120).

The WWTP of Sevres Anxaumont, is a small urban WWTP with a nominal capacity of 1,000 PE and with a sludge production of 4 tons DS/year. The sludge purged from the settling tank is sent alternatively to 4 reed beds every week. These reed beds were operated in 2002 and should be totally purged during 2015. Dried sludge and reeds are intended for agricultural soil amendment. The maturation process was monitored during 4 weeks. Samples were classified depending on their residence time (for example RB-1 corresponds to the reed bed actually feeded the week of sampling). Dewatered sludge were sampled on the surface of each reed bed (less than 50 cm depth) and closed to one inlet (maximum 1 meter).

The WWTP of Vivonne is a small urban plant treating WW collected from unitary network and exhibits a nominal capacity of 7,000 PE. After dewatering (15 % dry content), the sludge were dried into a greenhouse using solar energy. The sludge moved from the inlet to the outlet of the greenhouse thanks to a rotary scarifier which turned over and broke up the sludge. The sludge residence time in the greenhouse is about 1 month. Three samples were selected: a fresh sludge entering the greenhouse (Solar-0), at c.a. 15 days residence time (Solar-2w) and at the outlet of the greenhouse (Solar-4w, one month residence time).

2.2 Sample Preparation

All investigated samples were collected the same day (13th of January 2014, air temperature: 8°C, humidity: 85%) on the three WWTP, dried freeze (-50°C, 0.13 Pa) and stored at -20°C to avoid any change in biomass until analysis.

2.3 Global Analysis

2.3.1 Elemental Analysis

The OM content (i.e: mixed liquor volatile suspended solids) of WWS was determined from 3g sample, by combustion at 500°C for 4 h. Elemental analysis (C, H, N) was carried out on 1 mg sample using an elemental analyser (Thermo Electron Corporation Flash EA 1112 series) by catalytic combustion under oxygen at 970°C. To determine the sulfur percentage, 1 mg of vanadium oxide was added to 1 mg of the raw sludge.

2.3.2 Attenuated total reflectance Fourier transform infrared spectroscopy (ATR-FTIR)

ATR-FTIR spectra were recorded on a Thermo Nicolet 6700 Fourier transform infrared (FTIR) spectrometer equipped with a diamond crystal. Spectra were taken between 4000 and 650 cm^{-1} with a resolution of 4 cm^{-1}. 16 Scans were collected per spectrum.

Attenuated total reflectance or diffuse reflectance infrared transform infrared spectroscopy have been used to characterise or monitor the transformations of different fractions of organic matter of environmental samples such as composts or sewage sludge. Attenuated total reflectance Fourier transform infrared spectroscopy (ATR-FTIR) is indeed more appropriate than transmission infrared (IR) for the spectral characterisation of solid samples such as sewage sludge, as it provides a better resolution.

2.3.3 Organic matter fractionation

The OM was fractionated according to the method recommended by the International Humic Substances Society (so named IHSS) (Calderoni and Schnitzer 1984) from 10 g WWS. Lipids were extracted with 3 x 240 mL dichloromethane/methanol (2/1) using a Speed Extractor (Buchi). The extraction temperature was set to 80°C, nitrogen pressure was 50 bar, and the solvent contact time with the sample was 5 min. “Humic” and “fulvic acids” were extracted from the residue by 0.1 M NaOH (10 mL per g) under a nitrogen atmosphere in order to prevent OM oxydation. “Humic acids” were separated from “fulvic acids” by acidification to pH 1 (1 M HCl solution) and centrifugation (20 min, 8000 g). The alkaline-insoluble residue corresponded to “humin”.

2.4 Thermochemolysis (THM-GC/MS)

GC separations were done using a capillary column (30 m long, 0.25 mm i.d., 0.25 µm phase thickness). The injector temperature was set at 250°C. Column temperature was programmed from 50 to 300 °C at a rate of 5 °C.min^{-1} and then kept at 300 °C for 9 min. The ionization mode was electron impact (70 eV) and the source temperature was 220 °C.

Thermochemolysis was done using tetramethyl ammonium hydroxide (TMAH) as alkylating agent. 0.5 mg of lipids were mixed with 5 µL of TMAH methanolic solution 50/50 (v/v) in methanol and then placed in an inox cup. Thermochemolysis was realised using a temperature ramp from 100 °C to 350 °C with a temperature increase of 500 °C.min^{-1}.

The organic compounds were identified on the basis of their GC retention times and by comparison of their mass spectra with those of standards and library data (NIST).

Quantification was done using calibration standards (hexadecanoic acid, coprostanol and styrene) as describe by Collard et al. (2015).

Table 1: Limit of detection (LOD), limit of quantification (LOQ), linear regression and linearity factor (R2) for the 3 calibration standards

Standard	**LOD (µg)**	**LOQ (µg)**	**Linear regression**	**R^2**
Hexadecanoic acid	0.2	1.3	y=3171329x-2709871	0.98
Coprostanol	0.1	0.7	y=850765x-817706	0.99
Styrène	0.3	1.9	y=131582041x-55891604	0.99

3. Results and discussion

3.1 Thermal drying

The activated sludge (LF-0) was sampled in La Folie WWTP. At the end of WWT, the sludge is dried at 85°C (LF-85) to reduce water amount thus reducing the volume. After a first drying step at 85°C (LF-85), sludge is dried, sanitised and pelletised at 120 °C (LF-120).

Table 2: Elemental analysis of activated sludge and thermally dried sludge

	C +/- 12 (mg/g)	H +/- 2 (mg/g)	N +/- 3 (mg/g)	S (mg/g)	O +/- 14 (mg/g)*	O/C^a	C/N^a	H/C^b
LF 0	353	44	60	< LOQ	543	1.5	5.9	1.5
LF-85	362	55	63	< LOQ	520	1.4	5.7	1.8
LF-120	384	57	67	< LOQ	492	1.3	5.7	1.8

a : massic ratio; b : atomic ratio

*by difference

The organic matter content (table 3) and elemental composition (table 2) of LF-0 are in agreement with those previously determined for activated sludge [1].

The O/C and C/N ratios which are respectively linked with oxidation and biodegradability (Som et al. 2009) remained stable (table 2) during the thermal drying process.

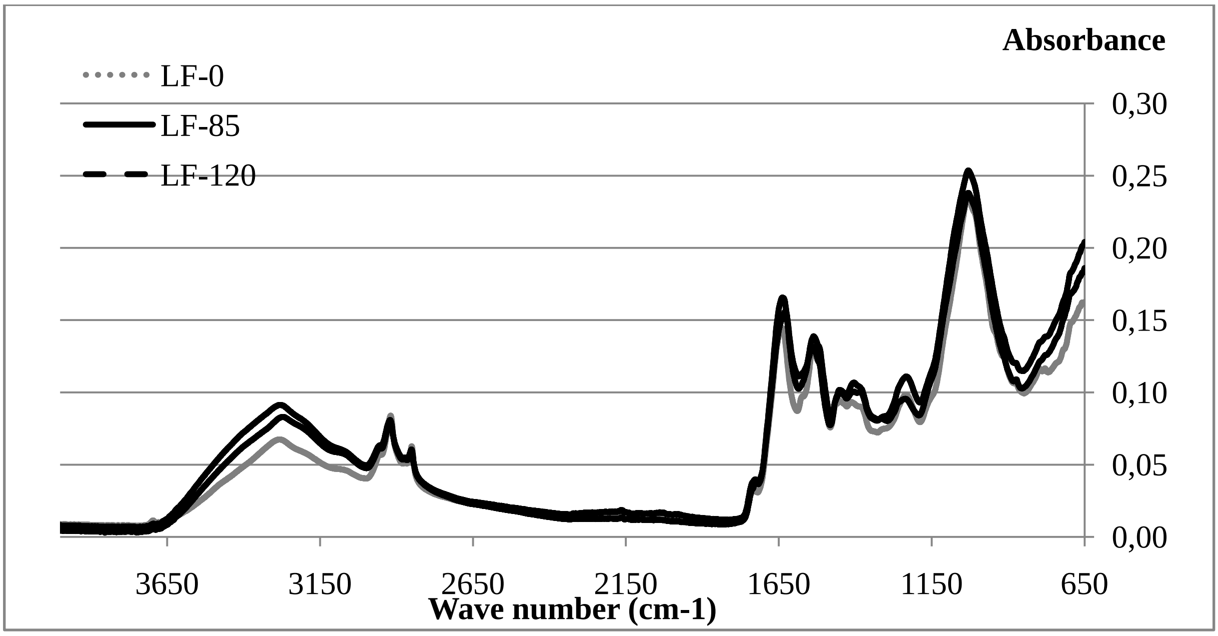

Figure 1: ATR-FTIR of raw sludge obtained by Thermal drying process (normalized to C-H bond (2925 cm-1))

ATR-FTIR spectra (figure 1) exhibited the following peaks wave numbers: 3270 cm^{-1} (OH stretch), 3180 cm^{-1} (NH_2 stretch of amides) (Smidt and Meissl 2007), 2925 cm^{-1} and 2855 cm^{-1} (aliphatic C-H stretch), 1630 cm^{-1} (O-H bond), 1540 cm^{-1} (C=O of amides) (Grube et al. 2006), 1250 cm^{-1} (C-O of carboxylic acids or C-N of amides), 1030 cm^{-1} (C-O stretch of polysaccharides) [6, 7].

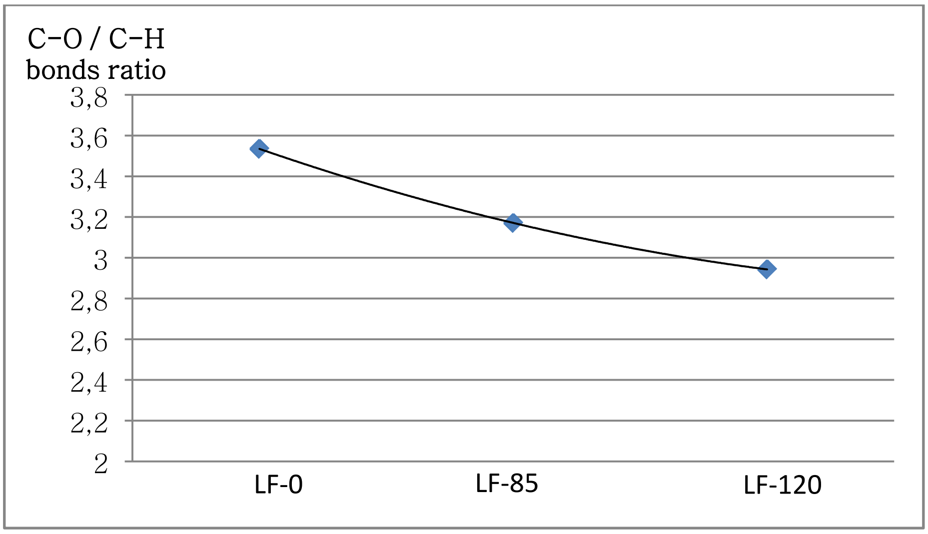

Figure 2: Evolution of C-O/C-H ratio during thermal drying process obtained by ATR-FTIR

The C-O/C-H ratio (figure 2), which allows the monitoring of OM oxidation, decreased with increasing drying temperatures. This traduces the predominance for reduction process.

The total OM content of WWS remained constant during the process (table 1). However the fractionation of OM before and after thermal drying showed a clear increase in lipids, fulvic acids and humic acids (table 3). In parallel, a strong decrease in humin-like fraction is observed. These changes are probably due to a weakening of OM. Lipidic compounds which were bound to the macromolecular network (Gobé et al. 2000) via ester, or ether bonds were probably released during this period thus increasing the extractable fractions. Such a desorption has already been observed in soil as the equilibrium was perturbed (Ambles et al. 1997).

Table 3: OM fractions of thermally dried samples

	OM +/- 40 (mg/g)	Lipids (mg/g)	« Fulvic acids » (mg/g)	« Humic acids » (mg/g)	« Humin » (mg/g)
LF 0	680	71.7	254.7*	83.1	590.4
LF-85	659	84.2	252.7*	69.2	593.8
LF-120	746	149.1	414.3*	135.2	301.4

*obtained by difference

The molecular analysis of the lipidic fraction was performed by THM-GC/MS (sup. Table S1). The same molecules were detected all along the process with stanols, sterols and fatty acids as main compounds. An increase of respectively 27% and 73% for acids and steroids is observed for LF-85 followed by a decrease of respectively 29% and 50% for acids and steroids for LF-120. As observed by Gobé et al. 2000, it is highly probable that polycyclic alcohols (stanols and sterols) and fatty acids were linked to the macromolecular network of polar lipids by ether and ester bonds. In the first stage of thermal drying (LF-85) these bonds could have been broken leading to an increase in stanols, sterols and fatty acids. These released compounds were degraded in the second stage of drying (LF-120).

The branched (iso+anteiso) to linear fatty acids ratio (table 4), decreased along the process demonstrating that the drying process has an inhibiting effect on bacterial activity (Guignard et al. 2005). Moreover the relative increase in stanols versus sterol traduces reducing conditions which are not favourable to bacterial activity.

Table 4: Evolution of stanols to sterol and branched to linear ratios during thermal drying

		LF-0	LF-85	LF-120
Steroids	Stanols / sterol	4.26	4.82	4.95
Fames	Branched / linear	2.43	2.30	2.12

Alkyl benzenes, phenolic compounds and indoles were observed in concentrations below the quantification limits (Sup table S1). These compounds are generally attributed to lignin therefore pyrolysis of microalgae also produces phenols, aromatic compounds and indoles which are attributed to proteins (Kebelmann et al. 2013).

The thermal drying induces a weakning of WWSs OM resulting in an increase in lipid, humic acids and fulvic acids amounts (LF-85) and a decrease in the insoluble fraction of OM (“humin”).

3.2 Solar drying

The first sample (Solar-0) which corresponds to the first step of the process, is the activated sludge sampled in Vivonne WWTP. At the end of the WWT, that sludge is introduced by underground pipes into a greenhouse to reduce water amount thus reducing the volume. During this drying process lasting a month long, sludge were sampled after 2 (Solar-2w) and 4 (Solar-4w) weeks residence time.

The pH slightly decreased (from 7.4 to 6.6) during the solar drying process due to the release of CO_2 during bacterial activity, as demonstrated by Pereira Lima (Pereira Lima et al. 2012). In contrast and according to measurement errors, OM content (table 6) and elemental composition (table 5) were not influenced by the drying period.

Table 5: Elemental analysis of activated sludge and solar dried sludge

	C +/- 12 (mg/g)	H +/- 2 (mg/g)	N +/- 3 (mg/g)	S (mg/g)	O +/- 14 (mg/g)*	O/C[a]	C/N[a]	H/C[b]
Solar-0	303	45	57	< LOQ	585	1.9	5.3	1.8
Solar-2w	332	49	54	< LOQ	555	1.7	6.1	1.8
Solar-4w	286	41	48	< LOQ	615	2.1	6.0	1.7

a : massic ratio; b : atomic ratio

*by difference

The total carbon content demonstrated a small variance between 2w and 4w (Table 5). This reduction may have occurred because of the use of carbon in the metabolic process of microorganisms, and correlated with the pH decrease as CO_2 is released. The average concentration obtained by Comparini (Pereira Lima et al. 2012) was 280 mg/g at the end of drying of the anaerobically digested sludge in a greenhouse, which confirm the results of elemental analysis. As observed during thermal drying, the O/C ratio remained stable during solar drying, whereas the C/N ratio went up a bit traducing an increase in biodegradability of the sludge at the end of the drying process.

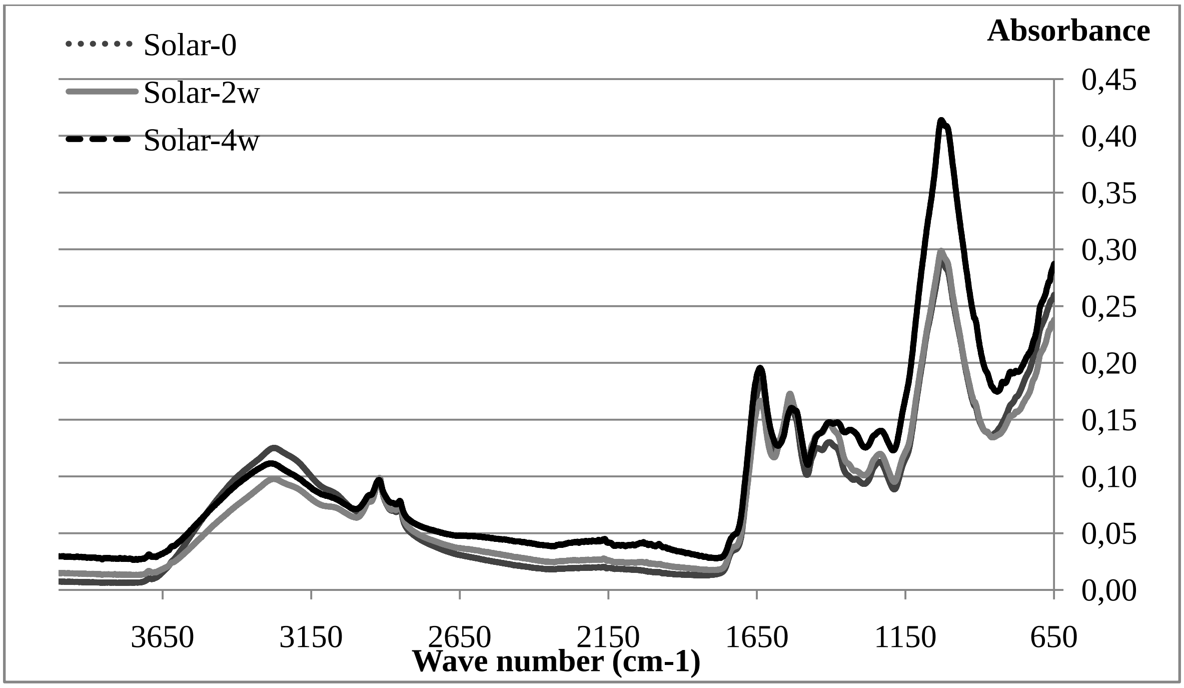

Figure 3: ATR-FTIR of raw sludge obtained by Solar drying process (normalized to C-H bond (2925 cm-1))

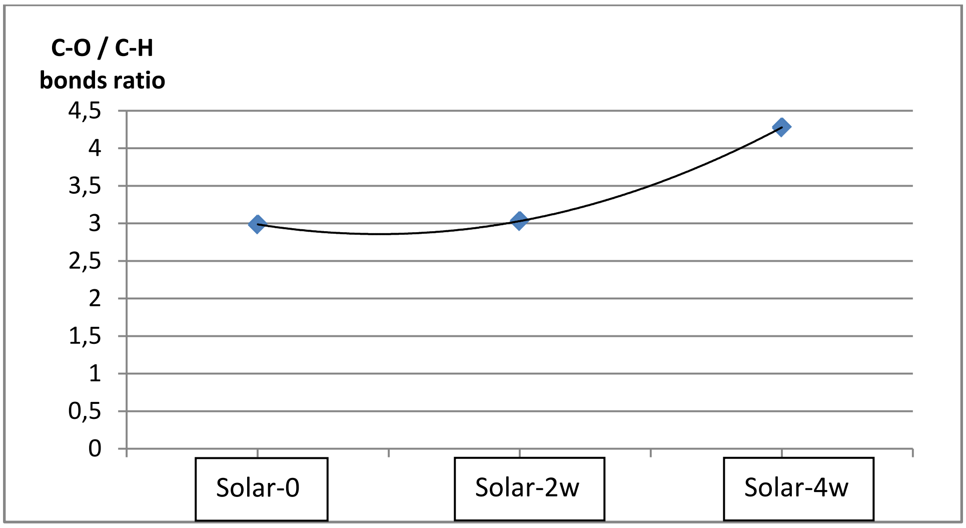

Figure 4: Evolution of C-O/C-H bonds ratio during solar drying process (ATR-FTIR)

ATR-FTIR spectra (fig. 3) resemble those observed for thermal drying process. However, the intensities of peaks varied during the drying processes. The C-O to C-H ratio climbed slightly (fig. 4) traducing an oxidation process.

A light increase in lipids (8%) is observed for the first period of drying (table 6), which can be due to a weakening of OM. This is followed by a strong decrease for the second stage of drying. This reduction in lipid amount can be related to an extent in microbial activity leading to the biodegradation of the organic content. Humification can also be responsible of such a decrease. Indeed, humic-like fractions, especially humic acids, increase in the second part of the solar drying process (table 6).

Table 6: OM fractions of solar dried samples

	OM +/- 40 (mg/g)	Lipids (mg/g)	« Fulvic acids » (mg/g)	« Humic acids » (mg/g)	« Humin » (mg/g)
Solar-0	630	70.7	372.4*	39.2	517.7
Solar-2w	667	76.4	329.2*	15.1	581.2
Solar-4w	627	42.9	333.9*	32.6	590.6

*obtained by difference

The total dried sludge and the lipid extracts were characterised at the molecular level using thermochemolysis at 350°C (THM).

Table 7: Compounds identified by THM-GCMS of raw sludge and lipids (mg/g)

	THM sludge			THM lipids		
	Solar-0	Solar-2w	Solar-4w	Solar-0	Solar-2w	Solar-4w
Total steroids	44.1	37.6	31.3	44.09	37.55	31.34
Total fatty acids *	127.7	130.0	97.8	127.67	130.02	97.77

*detected as FAMEs

As observed for thermal drying, THM of raw sludge and of lipids from solar drying mainly released steroids and fatty acids (as methyl esters) (table 7). The quantification of the THM products from both the total sludge and lipids conducted to very close results (Sup table S2). This indicates that, at 350°C, the insoluble OM does not contribute to the THM products, which were released, from the lipidic part of organic matter.

Despite the fact that the quantified THM products from lipids decreased, the relative percentage of the 2 class of compounds (22% steroids and 88% fatty acids) remains stable during the drying process (Sup table 2).

Table 8: Evolution of molecular parameters during the solar drying process

	Ratios	Solar-0	Solar-2w	Solar-4w
Steroids	Stanols / sterol	5.08	4.85	5.00
Fames	Branched / linear	2.17	2.21	2.20

There was no important change in the molecular composition of fatty acids. Indeed the branched (iso+anteiso) to linear fatty acids ratio remained stable (table 8) as well as the even to odd fatty acids ratio. As branched fatty acids are of bacterial origin whereas long even chained fatty acids are of plant origin one can see that there is no change in molecular inputs.

A decrease in fatty acids, stanols and sterols (Sup table 2) was observed for the second step (Solar-4w) which correlates with the strong decrease in lipids (table 6). As the decrease in lipids corresponds to a decrease in Carbon (table 5) and in OM content (table 6) it can be concluded that this trend is due, in part, to biodegradation.

3.3 Reed beds drying

The concentrated activated sludge (RB-0) was sampled in Sèvres Anxaumont (France) reed beds drying process. At the end of WWT, RB-0 is introduced by underground pipes into an outdoor tank containing reed beds. The aim is to reduce the volume of sludge by removing water. This drying process lasts generally ca. 10 years after which the sludge can be used in landfarming. Sludge is spread into 8 different tanks by a circular planning, each basin being supplied for a week before moving to the next. RB-1, 2, 3, and 4 correspond to sludge sampled in tanks which have been filled respectively 1, 2, 3 and 4 weeks before.

Table 9: Elemental analysis of activated sludge and dried sludge

	C +/- 12 (mg/g)	H +/- 2 (mg/g)	N +/- 3 (mg/g)	S (mg/g)	O +/- 14 (mg/g)*	O/C[a]	C/N[a]	H/C[b]
RB-0	335	44	62	< LOQ	559	1.7	5.4	1.6
RB-1	283	44	45	< LOQ	628	2.2	6.3	1.9
RB-2	264	45	43	< LOQ	648	2.5	6.1	2.0
RB-3	332	44	58	< LOQ	566	1.7	5.7	1.6
RB-4	335	49	54	< LOQ	562	1.7	6.2	1.8

a : massic ratio; b : atomic ratio LOQ : limit of quantification

*by difference

The OM content remains stable during the process, taking into account observational errors, with an amount of ca. 650 mg/g in RB-4 (table 10). The pH values slightly increase during the reed beds drying process (from 6.6 to 7.2 for the fresh (RB-0) and dried sludge (RB-4), respectively). The total carbon content demonstrated a small increase between the initial and final values (table 9). However the statistical results show that, at a significance level of 4%, there is no difference between initial and final carbon content in sample from reed beds drying. The increase may have occurred because of the degradation of reeds roots, incorporated in sampled sludge. It is also interesting to notice that the increase in nitrogen content is correlated with the decrease in oxygen content, which could be explained by reeds contribution (Gustavsson and Engwall 2012).

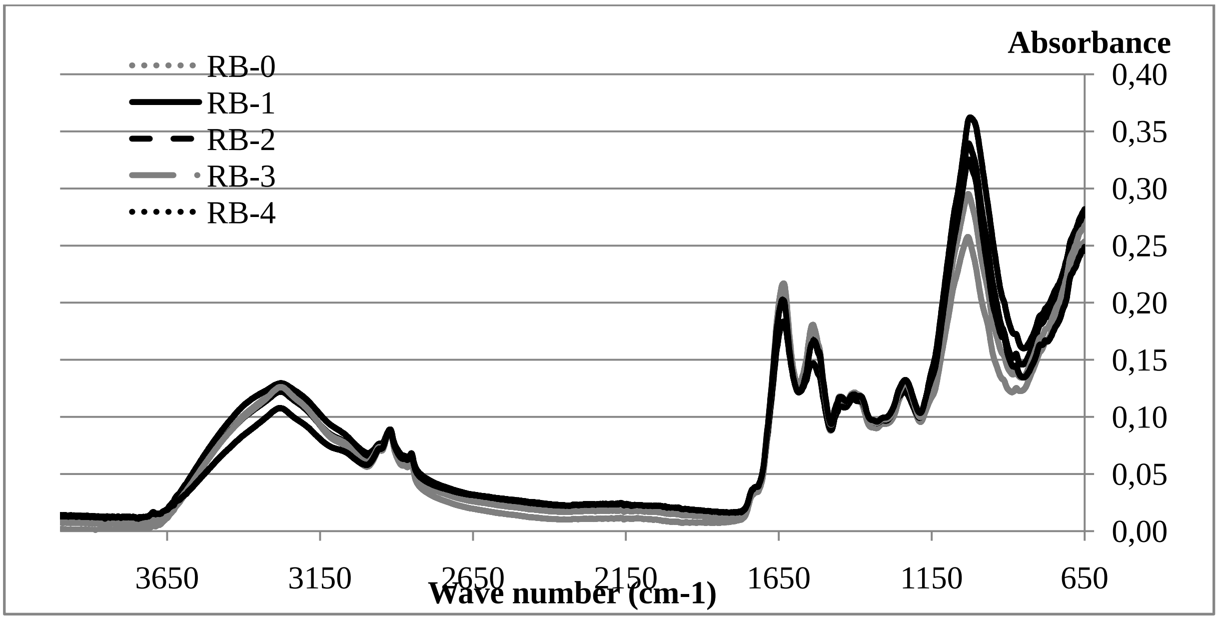

Figure 5: ATR-FTIR of raw sludge obtained by Reed beds drying process (normalized to C-H bond (2925 cm-1))

The C/O, C/N and H/C ratios (table 9) did not show significant variation, so one cannot conclude about the changes in degradability of OM during reed beds drying.

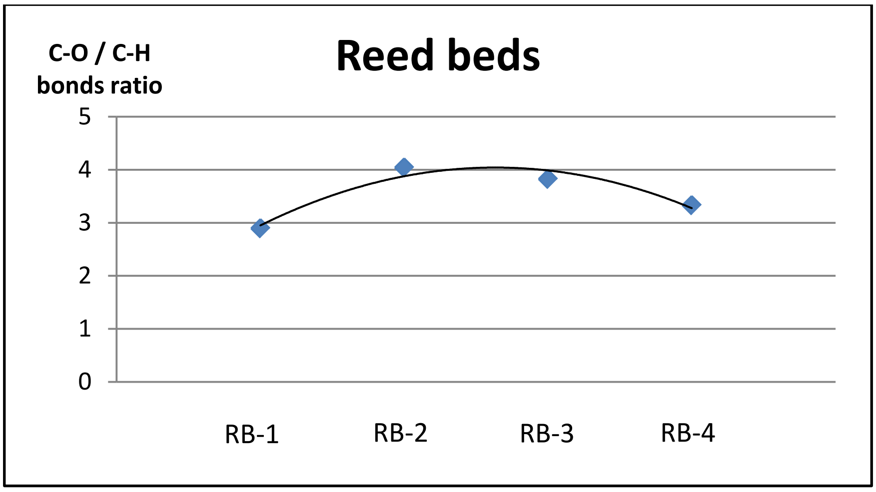

Figure 6: Evolution of C-O/C-H bonds ratio during reed beds drying (IR-FTIR)

A slight increase in C-O to C-H ratio (figure 6) can be observed at the beginning of the drying process followed by a less significant decrease. This result could be correlated with the increase in lipids observed within the first part of drying.

Contrarily to the IR ratio, the amount of lipids increased during the whole drying process (table 10). The amount of total humin-like substances did not vary, but humic acids decreased in a first time (RB-1 to RB-2) then remained stable until the end of the process. Contrarily to the two previous processes, it is not possible to correlate, for reed beds, the changes in lipids with humic substances.

Table 10: OM fractions of solar reed beds dried samples

	OM +/- 40 (mg/g)	Lipids (mg/g)	« Fulvic acids » (mg/g)	« Humic acids » (mg/g)	« Humin » (mg/g)
RB-0	620	62.9	431.7*	45.7	522.6
RB-1	680	46.3	369.1*	16.9	567.7
RB-2	690	63.5	300.1*	7.0	629.3
RB-3	670	73.8	391.3*	11.0	523.8
RB-4	650	81.8	347.7*	12.1	558.4

*By difference

In contrast and according to measurement errors, OM content slightly decreased by the drying period (RB-1 to RB-4). Lipids increased from 46.3 to 81.8 ‰ all along the process (table 10). The higher lipids content was found for the driest sludge sample, i.e. the one in contact with reed roots since a longer period.

THM-GCMS of reed beds sludge produced steroids and fatty acids as observed for the previous processes (Sup table S3). The total amount of detected compounds slightly decreased in the first step of reed beds drying and remained constant afterward. However some changes in compounds proportion were observed. The steroids amount is correlated with the lipid content contrarily to fatty acids.

Table 11: Representative ratio to evaluate OM of raw sludge evolution during reed beds drying

	Ratios	RB-0	RB-1	RB-2	RB-3	RB-4
Steroids	Stanols / sterol	4.89	4.54	4.74	4.93	4.57
Fames	Branched / linear	2.13	2.13	2.25	2.11	2.26
	Short / long	1.54	1.46	1.42	1.27	1.42

The stanols over sterol ratio (table 11) showed no evolution during the reed beds drying process, contrarily to the thermal drying process (table 4), which induced an increase in stanols evolution. The branched over linear fatty acids ratio (table 11) showed a slight increase during the dewatering mechanism. The short over long fatty acid ratio which is used to express the plant contribution as long even fatty acids originate from higher plants, showed no significant evolution during reed beds drying process. Contrarily to thermal and solar drying, reed beds drying doesn’t induce change in OM. This is not surprising since in this process fresh OM is regularly added to the sediment.

4. Conclusions

The OM of WWS submitted to 3 drying processes has been characterised at the global and molecular scales using elemental analysis, infra-red spectroscopy and thermochemolysis.

Before the drying step, the 3 studied WWS presented the same spectroscopic and molecular characteristics. The molecular characterisation of reed beds traduces no clear changes. However, this study puts in evidence the strong influence of solar and thermal drying processes on OM. Indeed, thermal drying induced a weakening of OM which is traduced by an increase in lipids concomitant with a decrease in “humin”. At the contrary, after 4 weeks of solar drying, the strong increase in humic-like substances in parallel with a decrease in lipids traduced the complexification of OM.

Our results showed that drying which reduces the volume of WWS thus lowering its cost of management, but change in OM characteristics can have an impact on the choice of WWS disposal. Indeed, solar drying which leads to an humified material should be favored for long term OM input (amendment) in land farming use, whereas thermally dried sludge aim to be used as fertilizer.

Acknowledgements

The research was financially supported by the French Ministère de l’Enseignement Supérieur et de la Recherche.

References

Ambles A, Lemee L, Jambu P, Mayoungou-Vembet P (1997) Equilibrium between free and bound lipids in a rendzina soil in natural conditions and with laboratory disturbances. Agrochimica 41, 196–208.

Bux M, Baumann R, Quadt S, et al (2002) Volume reduction and biological stabilization of sludge in small sewage plants by solar drying. Drying Technology 20, 829.

Calderoni G, Schnitzer M (1984) Effects of age on the chemical structure of paleosol humic acids and fulvic acids. Geochimica et Cosmochimica Acta 48, 2045–2051.

Chai LH (2007) Statistical dynamic features of sludge drying systems. International Journal of Thermal Sciences 46, 802–811.

Commission of European Communities Council Directive 91/271/EEC of 21 March 1991 concerning waste-water treatment (amended by the 98/15/EC of 27 February 1998).

Edwards JK, Gray KR, Cooper DJ, et al (2001) Reed bed dewatering of agricultural sludges and slurries. Water Science And Technology, A Journal Of The International Association On Water Pollution Research 44, 551–558.

Filip Z, Bielek P (2002) Susceptibility of humic acids from soils with various contents of metals to microbial utilization and transformation (English). Biology and fertility of soils 36, 426–433.

Gao N, Li J, Qi B, et al (2014) Thermal analysis and products distribution of dried sewage sludge pyrolysis. Journal of Analytical and Applied Pyrolysis 105, 43–48.

Gobé V, Lemée L, Amblès A (2000) Structure elucidation of soil macromolecular lipids by preparative pyrolysis and thermochemolysis. Organic Geochemistry 31, 409–419.

González-Vila FJ , Amblès A , del Río JC , L. G (2001) Characterisation and differentiation of kerogens by pyrolytic and chemical degradation techniques. Journal of Analytical and Applied Pyrolysis 58–59, 315–328.

Grube M, Lin JG, Lee PH, Kokorevicha S (2006) Evaluation of sewage sludge-based compost by FT-IR spectroscopy. Geoderma 130, 324–333.

Guignard C, Lemée L, Amblès A (2005) Lipid constituents of peat humic acids and humin. Distinction from directly extractable bitumen components using TMAH and TEAAc thermochemolysis. Organic Geochemistry 36, 287–297.

Gustavsson L, Engwall M (2012) Treatment of sludge containing nitro-aromatic compounds in reed-bed mesocosms – Water, BOD, carbon and nutrient removal. Waste Management 32, 104–109.

Hernández T, Moral R, Perez-Espinosa A, et al (2002) Nitrogen mineralisation potential in calcareous soils amended with sewage sludge. Bioresource Technology 83, 213–219.

Jardé E, Mansuy L, Faure P (2003) Characterization of the macromolecular organic content of sewage sludges by thermally assisted hydrolysis and methylation-gas chromatography–mass spectrometer (THM-GC/MS). Journal of Analytical and Applied Pyrolysis 68–69, 331–350.

Jardé E, Mansuy L, Faure P (2005a) Organic markers in the lipidic fraction of sewage sludges. Water Research 39, 1215–1232.

Jardé E, Mansuy L, Faure P (2005b) Organic markers in the lipidic fraction of sewage sludges. Water Research 39, 1215–1232.

Kebelmann K, Hornung A, Karsten U, Griffiths G (2013) Intermediate pyrolysis and product identification by TGA and Py-GC/MS of green microalgae and their extracted protein and lipid components. Biomass and Bioenergy 49, 38–48.

Kelessidis A, Stasinakis AS (2012) Comparative study of the methods used for treatment and final disposal of sewage sludge in European countries. Waste Management 32, 1186–1195.

Kwon EE, Yi H, Kwon HH (2013) Urban energy mining from sewage sludge. Chemosphere 90, 1508–1513. doi, 10.1016/j.chemosphere.2012.07.062

Lasaridi KE, Stentiford EI (1998) A simple respirometric technique for assessing compost stability. Water Research 32, 3717–3723.

Mathioudakis VL, Kapagiannidis AG, Athanasoulia E, et al (2013) Sewage Sludge Solar Drying, Experiences from the First Pilot-Scale Application in Greece. Drying Technology 31, 519–526.

Nassar AM, Smith M, Afifi S (2006) Sludge dewatering using the reed bed system in the Gaza Strip, Palestine. Water & Environment Journal 20, 27–34.

Nielsen S [b1] (analytic) (2003) Sludge drying reed beds. Water Science and Technology 48, 101–109.

Nielsen S, Willoughby N (2005) Sludge treatment and drying reed bed systems in Denmark. Water & Environment Journal 19, 296–305.

Parnaudeau V, Dignac M-F (2007) The organic matter composition of various wastewater sludges and their neutral detergent fractions as revealed by pyrolysis-GC/MS. Journal of Analytical and Applied Pyrolysis 78, 140–152.

Pereira Lima MR, Zandonade E, Sobrinho PA (2012) Characteristics of WWTP sludge after drying in greenhouse for agricultural purposes. Water Science & Technology 66, 1460–1466.

Pognani M, Barrena R, Font X, et al (2011) Evolution of organic matter in a full-scale composting plant for the treatment of sewage sludge and biowaste by respiration techniques and pyrolysis-GC/MS. Bioresource Technology 102, 4536–4543.

Réveillé V, Mansuy L, Jardé É, Garnier-Sillam É (2003) Characterisation of sewage sludge-derived organic matter, lipids and humic acids. Organic Geochemistry 34, 615–627.

Senesi N, D’Orazio V, Ricca G (2003) Humic acids in the first generation of EUROSOILS. Geoderma 116, 325–344.

Silva MEF, de Lemos LT, Nunes OC, Cunha-Queda AC (2014) Influence of the composition of the initial mixtures on the chemical composition, physicochemical properties and humic-like substances content of composts. Waste Management 34, 21–27.

Smidt E, Meissl K (2007) The applicability of Fourier transform infrared (FT-IR) spectroscopy in waste management. Waste Management 27, 268–276.

Som M-P, Lemée L, Amblès A (2009) Stability and maturity of a green waste and biowaste compost assessed on the basis of a molecular study using spectroscopy, thermal analysis, thermodesorption and thermochemolysis. Bioresource Technology 100, 4404–4416.

Uggetti E, Ferrer I, Llorens E, García J (2010) Sludge treatment wetlands, A review on the state of the art. Bioresource Technology 101, 2905–2912.

Council Directive 1999/30/EEC of 22 April 1999 relating to waste incineration.

Tables Caption

Table 12: Limit of detection (LOD), limit of quantification (LOQ), linear regression and linearity factor (R2) for the 3 calibration standards

Table 13: Elemental analysis of activated sludge and thermally dried sludge

Table 14: OM fractions of thermally dried samples

Table 15: Evolution of stanols to sterol and branched to linear ratios during thermal drying

Table 16: Elemental analysis of activated sludge and solar dried sludge

Table 17: OM fractions of solar dried samples

Table 18: Compounds identified by THM-GCMS of raw sludge and lipids (mg/g)

Table 19: evolution of molecular parameters during the solar drying process

Table 20: Elemental analysis of activated sludge and dried sludge

Table 21: OM fractions of solar reed beds dried samples

Table 22: Representative ratio to evaluate OM of raw sludge evolution during reed beds drying

Supplementary Tables Caption

Table S23: Molecular composition of lipidic fraction of sludge during thermal drying process

Table S24: Molecular composition of lipidic fraction of sludge during solar drying process

Table S25: Molecular composition of lipidic fraction of sludge during reed beds drying process

Figures caption

Figure 7: ATR-FTIR of raw sludge obtained by Thermal drying process (normalized to C-H bond (2925 cm-1))

Figure 8: Evolution of C-O/C-H ratio during thermal drying process obtained by ATR-FTIR

Figure 9: ATR-FTIR of raw sludge obtained by Solar drying process (normalized to C-H bond (2925 cm-1))

Figure 10: Evolution of C-O/C-H bonds ratio during solar drying process (ATR-FTIR)

Figure 11: ATR-FTIR of raw sludge obtained by Reed beds drying process (normalized to C-H bond (2925 cm-1))

Figure 12: Evolution of C-O/C-H bonds ratio during reed beds drying (IR-FTIR)

Identification number	Compouds names	Concentration (mg/g)		
		LF-0	LF-85	LF-120
L1	Toluene	< LOQ	< LOQ	< LOQ
L2	Ethylbenzene	< LOQ	< LOQ	< LOQ
L3	Styrene	< LOQ	< LOQ	< LOQ
L4	Phenol	< LOQ	< LOQ	< LOQ
L5	Methyl Phenol	< LOQ	< LOQ	< LOQ
L6	Benzyl nitrile	< LOQ	< LOQ	< LOQ
L7	Methoxy Benzaldehyde	< LOQ	< LOQ	< LOQ
L8	Indole	< LOQ	< LOQ	< LOQ
L9	Methyl Indole	< LOQ	< LOQ	< LOQ
S1	5β-Cholestan-3-ol.(OMe)	6.51	13.57	4.74
S2	5α-Cholestan-3-ol.(OMe)	1.77	2.99	2.49
S3	Cholesterol (OMe)	3.88	6.07	2.86
S4	Cholestanol (OMe)	2.57	3.92	2.23
S5	Ethyl cholestanol (OMe)	3.75	6.15	2.93
S6	Ethyl cholestanol (OMe)	1.94	2.59	1.78
F1	Hexanoic acid methyl ester	1.76	1.56	1.52
F2	Heptanoic acid methyl ester	1.22	1.18	1.17
F3	Octanoic acid methyl ester	1.57	1.32	1.71
F4	Nonanoic acid methyl ester	1.04	1.08	1.05
F5	Decanoic acid methyl ester	1.62	1.30	1.81
F6	Undecanoic acid methyl ester	1.10	1.27	1.22
F7	Dodecanoic acid methyl ester	3.32	2.98	3.90
F8	Tridecanoic acid methyl ester	2.16	1.58	2.17
F9	Tetradecenoic acid methyl ester	2.60	1.92	2.19
F10	Tetradecanoic acid methyl ester	7.72	7.68	6.35
F11	iso Pentadecanoic acid methyl ester	7.70	8.40	6.27
F12	anteiso Pentadecanoic acid methyl ester	3.40	3.76	3.07
F13	Pentadecanoic acid methyl ester	3.63	4.34	3.54
F14	Hexadecenoic acid methyl ester	2.36	4.40	1.53
F15	Hexadecanoic acid methyl ester	21.99	33.65	17.07
F16	iso Heptadecanoic acid methyl ester	2.38	2.02	2.28
F17	anteiso Heptadecanoic acid methyl ester	1.57	1.45	1.58
F18	Heptadecanoic acid methyl ester	2.57	2.45	2.67
F19	Octodecenoic acid methyl ester	3.16	8.51	4.30
F20	Octodecanoic acid methyl ester	9.11	17.31	7.83
F21	Nonadecanoic acid methyl ester	1.09	0.95	1.10
F22	Eicosanoic acid methyl ester	2.23	2.18	2.10
F23	Heneicosanoic acid methyl ester	1.09	1.06	1.08
F24	Docosanoic acid methyl ester	2.23	2.58	2.07
F25	Tricosanoic acid methyl ester	1.27	1.23	1.22
F26	Tetracosanoic acid methyl ester	2.09	2.45	1.83
F27	Pentasanoic acid methyl ester	1.14	1.13	1.06
F28	Hexacosanoic acid methyl ester	1.52	1.69	1.36
F29	Heptacosanoic acid methyl ester	0.94	0.95	0.92
F30	Octacosanoic acid methyl ester	1.18	1.27	1.12
F31	Triacontanoic acid methyl ester	1.06	1.12	1.04

Table S1 : Molecular composition of lipidic fraction of sludge during thermal drying process

Identification number	Compouds names	Concentration (mg/g) Solar-0	Solar-2w	Solar-4w
L1	Toluene	< LOQ	< LOQ	< LOQ
L2	Ethylbenzene	< LOQ	< LOQ	< LOQ
L3	Styrene	< LOQ	< LOQ	< LOQ
L4	Phenol	< LOQ	< LOQ	< LOQ
L5	Methyl Phenol	< LOQ	< LOQ	< LOQ
L6	Benzyl nitrile	< LOQ	< LOQ	< LOQ
L7	Methoxy Benzaldehyde	< LOQ	< LOQ	< LOQ
L8	Indole	< LOQ	< LOQ	< LOQ
L9	Methyl Indole	< LOQ	< LOQ	< LOQ
S1	5β-Cholestan-3-ol.(OMe)	17.83	13.58	9.99
S2	5α-Cholestan-3-ol.(OMe)	3.20	3.29	2.46
S3	Cholesterol (OMe)	7.94	7.12	5.57
S4	Cholestanol (OMe)	4.21	3.88	3.43
S5	Ethyl cholestanol (OMe)	7.95	6.83	6.76
S6	Ethyl cholestanol (OMe)	2.95	2.85	3.14
F1	Hexanoic acid methyl ester	1.52	2.71	1.31
F2	Heptanoic acid methyl ester	0.95	0.95	0.94
F3	Octanoic acid methyl ester	1.26	1.31	1.32
F4	Nonanoic acid methyl ester	0.99	0.99	0.98
F5	Decanoic acid methyl ester	1.40	1.55	1.24
F6	Undecanoic acid methyl ester	0.98	1.03	0.96
F7	Dodecanoic acid methyl ester	3.35	4.18	2.57
F8	Tridecanoic acid methyl ester	1.41	1.76	1.26
F9	Tetradecenoic acid methyl ester	2.05	2.23	1.87
F10	Tetradecanoic acid methyl ester	9.18	12.04	5.54
F11	iso Pentadecanoic acid methyl ester	7.97	8.21	6.82
F12	anteiso Pentadecanoic acid methyl ester	4.37	4.41	3.61
F13	Pentadecanoic acid methyl ester	3.94	4.43	2.81
F14	Hexadecenoic acid methyl ester	5.30	4.31	3.31
F15	Hexadecanoic acid methyl ester	33.26	33.46	20.03
F16	iso Heptadecanoic acid methyl ester	2.61	3.07	2.65
F17	anteiso Heptadecanoic acid methyl ester	1.78	1.96	1.70
F18	Heptadecanoic acid methyl ester	2.76	2.97	2.30
F19	Octodecenoic acid methyl ester	7.36	6.09	4.38
F20	Octodecanoic acid methyl ester	17.01	14.76	10.89
F21	Nonadecanoic acid methyl ester	1.03	1.04	1.24
F22	Eicosanoic acid methyl ester	2.70	2.64	2.41
F23	Heneicosanoic acid methyl ester	1.07	1.08	1.14
F24	Docosanoic acid methyl ester	2.83	2.68	3.14
F25	Tricosanoic acid methyl ester	1.34	1.33	1.58
F26	Tetracosanoic acid methyl ester	2.79	2.58	3.33
F27	Pentasanoic acid methyl ester	1.21	1.19	1.44
F28	Hexacosanoic acid methyl ester	1.84	1.78	2.46
F29	Heptacosanoic acid methyl ester	0.96	0.95	1.07
F30	Octacosanoic acid methyl ester	1.33	1.25	1.86
F31	Triacontanoic acid methyl ester	1.14	1.10	1.59

Table S2 : Molecular composition of lipidic fraction of sludge during solar drying process

		Concentration (mg/g)			
Identification number	Compouds names	RB-1	RB-2	RB-3	RB-4
L1	Toluene	< LOQ	< LOQ	< LOQ	< LOQ
L2	Ethylbenzene	< LOQ	< LOQ	< LOQ	< LOQ
L3	Styrene	< LOQ	< LOQ	< LOQ	< LOQ
L4	Phenol	< LOQ	< LOQ	< LOQ	< LOQ
L5	Methyl Phenol	< LOQ	< LOQ	< LOQ	< LOQ
L6	Benzyl nitrile	< LOQ	< LOQ	< LOQ	< LOQ
L7	Methoxy Benzaldehyde	< LOQ	< LOQ	< LOQ	< LOQ
L8	Indole	< LOQ	< LOQ	< LOQ	< LOQ
L9	Methyl Indole	< LOQ	< LOQ	< LOQ	< LOQ
S1	5β-Cholestan-3-ol.(OMe)	4.97	6.10	8.44	7.07
S2	5α-Cholestan-3-ol.(OMe)	1.61	2.16	1.93	2.39
S3	Cholesterol (OMe)	4.06	4.01	4.57	3.90
S4	Cholestanol (OMe)	2.34	2.81	3.01	3.39
S5	Ethyl cholestanol (OMe)	3.32	3.55	4.41	3.94
S6	Ethyl cholestanol (OMe)	1.85	2.01	1.95	2.23
F1	Hexanoic acid methyl ester	1.09	1.16	1.27	1.05
F2	Heptanoic acid methyl ester	0.93	0.95	1.01	0.91
F3	Octanoic acid methyl ester	1.13	1.26	1.25	1.07
F4	Nonanoic acid methyl ester	0.92	0.95	0.98	0.92
F5	Decanoic acid methyl ester	1.02	1.20	1.19	1.08
F6	Undecanoic acid methyl ester	0.95	1.09	1.12	1.04
F7	Dodecanoic acid methyl ester	1.74	2.48	2.60	1.93
F8	Tridecanoic acid methyl ester	1.11	1.49	1.48	1.33
F9	Tetradecenoic acid methyl ester	1.41	1.89	1.93	1.54
F10	Tetradecanoic acid methyl ester	3.80	5.83	5.85	4.39
F11	iso Pentadecanoic acid methyl ester	3.72	7.01	7.57	5.71
F12	anteiso Pentadecanoic acid methyl ester	2.23	3.68	3.72	2.92
F13	Pentadecanoic acid methyl ester	1.88	3.44	3.49	2.82
F14	Hexadecenoic acid methyl ester	2.49	3.59	3.98	3.11
F15	Hexadecanoic acid methyl ester	14.27	20.76	20.11	14.59
F16	iso Heptadecanoic acid methyl ester	1.70	2.17	2.16	1.80
F17	anteiso Heptadecanoic acid methyl ester	1.31	1.55	1.56	1.33
F18	Heptadecanoic acid methyl ester	1.59	2.09	2.09	1.71
F19	Octodecenoic acid methyl ester	4.85	4.94	5.22	4.10
F20	Octodecanoic acid methyl ester	7.03	10.54	10.84	7.67
F21	Nonadecanoic acid methyl ester	0.96	1.01	0.99	0.94
F22	Eicosanoic acid methyl ester	1.66	2.31	1.92	1.53
F23	Heneicosanoic acid methyl ester	1.07	1.12	1.12	1.04
F24	Docosanoic acid methyl ester	2.49	2.71	2.42	1.94
F25	Tricosanoic acid methyl ester	1.33	1.29	1.20	1.12
F26	Tetracosanoic acid methyl ester	2.52	2.61	2.19	1.89
F27	Pentasanoic acid methyl ester	1.20	1.23	1.09	1.06
F28	Hexacosanoic acid methyl ester	2.18	2.02	1.58	1.54
F29	Heptacosanoic acid methyl ester	0.99	1.00	0.93	0.93
F30	Octacosanoic acid methyl ester	1.61	1.50	1.19	1.22
F31	Triacontanoic acid methyl ester	1.39	1.34	1.10	1.11

Table S3 : Molecular composition of lipidic fraction of sludge during reed beds drying process